



1

Nonlinear Models and Behaviors of DC–DC Converters

1.1 Introduction

DC–DC converters are widely used in industrial and commercial applications with the requirement of regulating DC power, such as computers, spacecrafts, medical instruments, communication devices, electrical vehicles, and so on [1–6]. The technology of DC–DC conversion is a major subject area in the field of power engineering and drives, and has been under development for seven decades [5]. It is well known that DC–DC converters are typical nonlinear systems because of their switching processes. Some irregular behavior, such as subharmonics and intermittent instability, has been observed constantly in practice. Over nearly three decades, lots of nonlinear behavior, such as period-doubling bifurcation, Hopf bifurcation, border collision bifurcation, torus bifurcation, coexistence attractor, intermittent chaos and chaos, has been studied by power electronics researchers one after the other [7–17].

Although the nonlinear behavior of DC–DC converters has been intensively studied, people are still puzzled by the practical application of bifurcations and chaos in switching converters [18]. Miniaturization is the main approach to reduce the size of DC–DC converters, and a higher switching frequency must be utilized with the requirement of the smaller size. Electromagnetic interference (EMI), resulting from bursting changes of voltage or current (dv/dt or di/dt), has been a major design constraint for a long time due to the high switching frequency. The question of how to reduce annoying and harmful EMI has attracted much research interest.

Fortunately, chaos research opens up the possibility of the application of nonlinear characteristics in power electronic systems, and might be a new method to improve the performance of power electronic systems in the future. For example, the switching speed between unstable periodic orbits (UPOs) embedded in chaos attractors is fast. Using this performance, DC–DC converters working in chaos may have a fast dynamic response [19]. Moreover, it has been actually proved that the application of



chaotic power spectral characteristics can effectively reduce the EMI and improve the electromagnetic compatibility (EMC) of DC–DC converters [20–25].

Although spectrum analysis of chaotic switching converters has resulted in some research achievements, there are still fewer quantitative indicators and comprehensive assessments of the characteristics of the chaotic spectrum because the switching converter is a complex nonlinear, nonautonomous, and time varying system. First of all, we need to know about the nonlinear behavior of switching converters and some basic dynamical concepts. In this chapter, we will begin with an introduction to DC–DC converters and their operation modes. Next, the conventional modeling methods are presented. Some basic nonlinear dynamics knowledge is then introduced in the rest of this chapter.

1.2 Overview of PWM DC–DC Converters

1.2.1 Principle of Pulse Width Modulation

DC–DC converters supply a regulated DC output voltage to a variable-load resistance effectively. Switch-mode DC–DC converters convert one DC input voltage V_{in} to a desired output voltage V_{out} by storing the input energy temporarily and then releasing that energy to the output load. The average value of voltage is moderated by controlling the switch on and off durations (t_{on} and t_{off}). In Figure 1.1, the input voltage V_{in} is chopped to an output voltage V_{out} . The longer the switch is on compared to the off duration, the higher the power supplied to the load. So, the duty cycle, describing the ratio of on duration to the switching time period T , is defined as

$$d = t_{on}/T \quad (1.1)$$

Obviously, the average output voltage varies depending on d . By varying d , V_{out} can be controlled. So, this method is called *Pulse Width Modulation (PWM)*.

The simplest way to generate a PWM signal is by comparison, which requires only a sawtooth or a triangle waveform and a comparator. When the value of the control signal (v_{con} , the dash line, commonly comes from the error of the actual output voltage and reference voltage) is greater than the modulation waveform (v_{ramp} , the sawtooth with fixed frequency T and peak value V_U), the comparator output becomes high,

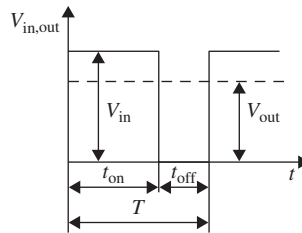


Figure 1.1 DC–DC converter voltage waveforms

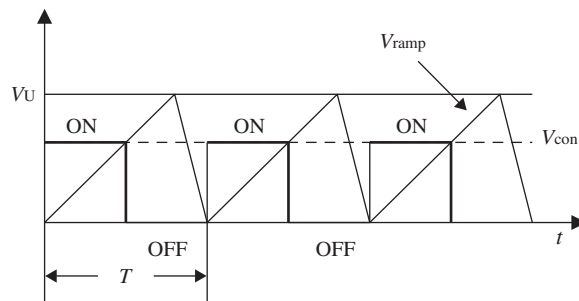


Figure 1.2 Pulse width modulation concept

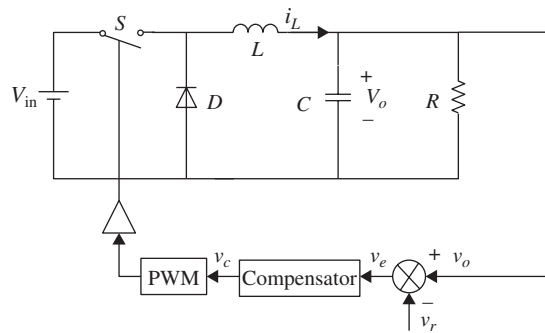


Figure 1.3 Closed-loop controlled PWM system to regulate the output voltage

otherwise it is in the low state shown in Figure 1.2 [4]. In practical terms, a PWM controller consists of three main components: a clock for setting the switching frequency, an output voltage error amplifier, and a sawtooth signal synchronized with the clock.

To illustrate, a PWM step-down converter and feedback loop block is shown in Figure 1.3 as an example. A closed-loop converter contains three ports: a switching main circuit, sampling circuit, and a control circuit that is introduced to regulate the output voltage. It is desired to design the feedback system in such a way that the output voltage is accurately regulated, and is insensitive to disturbances in v_g or in the load current [3]. A control system can be constructed by causing the output voltage to follow a given reference voltage by varying the duty cycle, because the output voltage is a function of the switch's duty cycle.

1.2.2 Basic Topologies of DC–DC Converters

According to incomplete statistics, there have been more than 500 prototypes of DC–DC converters developed over the past seven decades. But all of them come

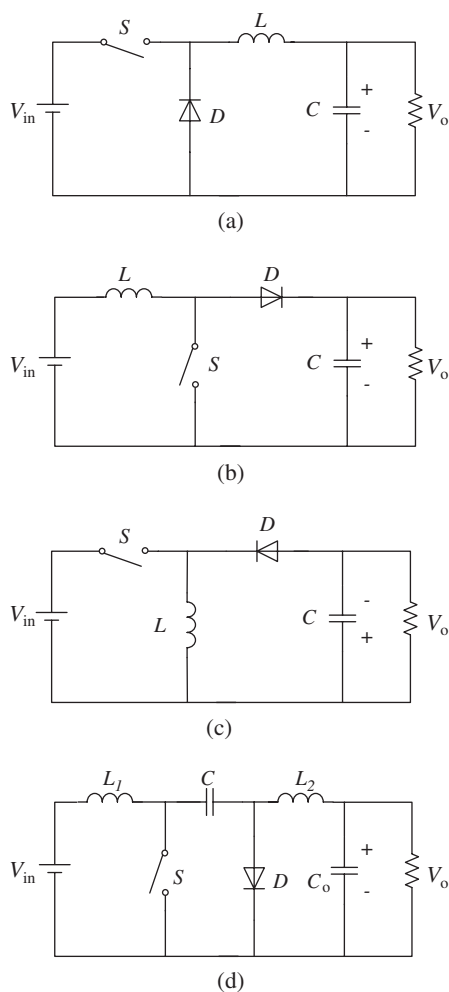


Figure 1.4 Basic topologies of nonisolated DC–DC converters including (a) buck, (b) boost, (c) buck–boost, and (d) Ćuk converters

from the several basic topologies shown in Figure 1.4, where switch S and diode D are alternately on and off. In these topologies, converters, are the two most basic topologies. The buck–boost converter carries out both the stepping up and down action. The Ćuk converter is a duality buck–boost converter.

If the output is required to be electrically isolated from the input, isolated DC–DC converters, whose isolation is provided by a high frequency isolation transform, are needed. There are two kinds of isolated topologies, unidirectional and bidirectional core excitation based on the way they use the transformer core. The unidirectional

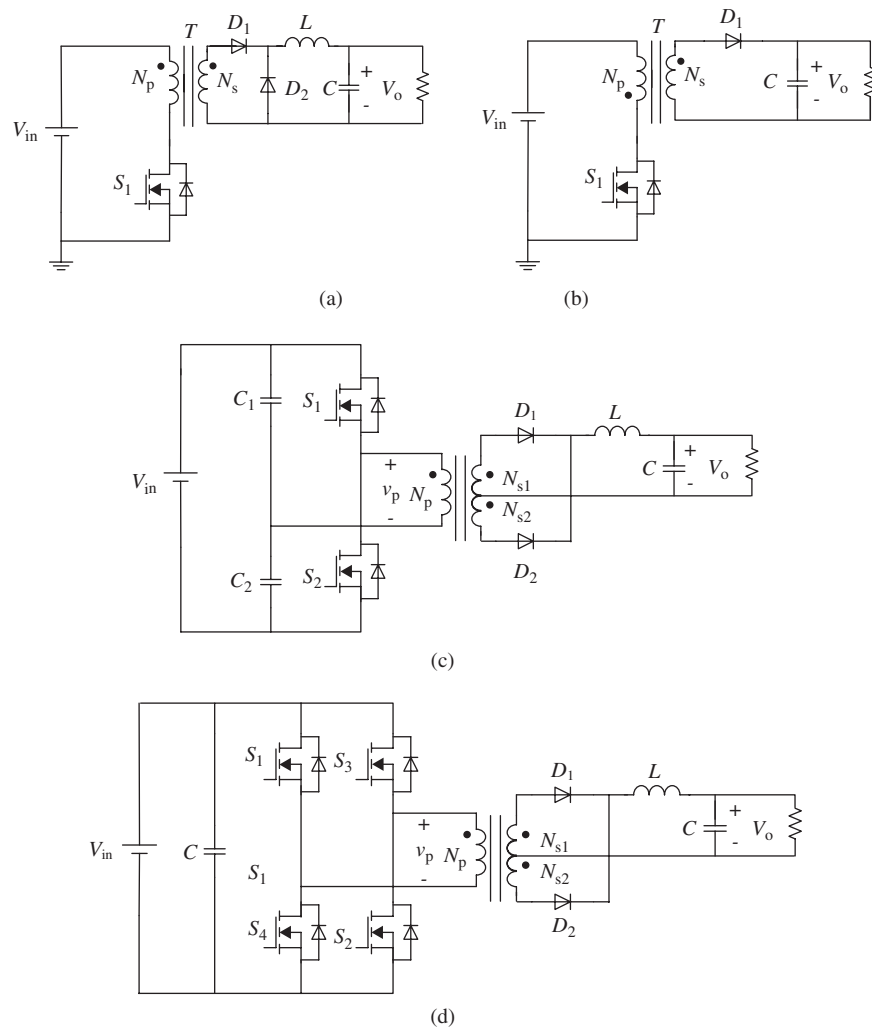


Figure 1.5 Isolated DC–DC converters including (a) forward, (b) flyback, (c) half-bridge, and (d) full-bridge converters

topology has two categories: forward converter and flyback converter, whose output voltages are regulated by means of the PWM scheme. The bidirectional topology has three categories: push-pull, half-bridge, and full-bridge. The circuits of forward, flyback, half-bridge and full-bridge converters are shown in Figure 1.5(a)-(d) respectively. Topologically, the flyback converter is an isolated buck–boost converter, and the half-bridge and full-bridge are isolated buck converters.



1.2.3 Operation Modes of DC-DC Converters

DC-DC converters operate in one of two modes depending on the characteristics of the inductor current [2, 4]:

1. *continuous conduction mode (CCM)*,
2. *discontinuous conduction mode (DCM)*.

As shown in Figure 1.6, the continuous conduction mode is defined by the continuous output current (greater than zero) over the entire switching period, whereas the DCM is defined by the discontinuous output current (equal to zero) during any portion of the switching period. Each mode is discussed in relation to the buck-boost converters in subsequent sections [4].

1.2.3.1 Continuous Conduction Mode

The operation of CCM in steady state consists of two states – switch-on and switch-off modes – whose equivalent circuits of boost converter are illustrated in Figure 1.7. When the switch is on for a time duration t_{on} , the switch conducts the source power and the diode becomes reverse biased, then the inductor current linearly increases. When the switch is off for a time duration t_{off} , the diode becomes forward biased, and the inductor current increases.

1.2.3.2 Discontinuous Conduction Mode

The operation of DCM in steady state consists of three states besides the two modes mentioned above, and the third one is that S and D are all off and the inductor current

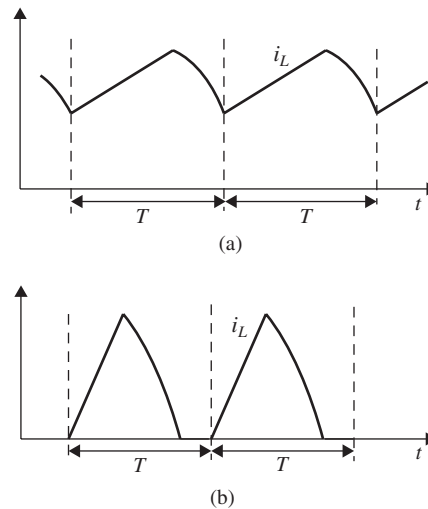


Figure 1.6 Inductor current waveforms at (a) CCM and (b) DCM

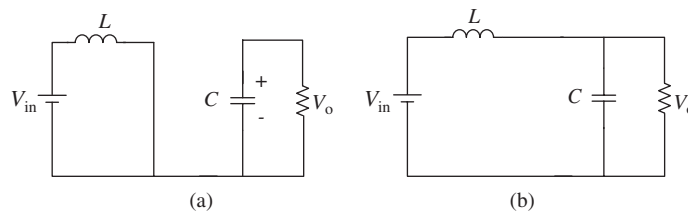


Figure 1.7 CCM circuit states of boost converter when (a) S on, D off and (b) S off, D on

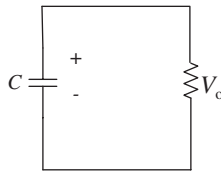


Figure 1.8 DCM circuit state of boost converter (S off, D off)

stays zero. Figure 1.8 shows the waveforms for the DCM. In this mode, the inductor current drops all the way to zero some time after the switch is turned off, and then remains at zero, with the transistor and diode both off, until the transistor is turned on again.

1.2.4 State-Space Model of DC–DC Converters

A feedback controlled buck converter is illustrated in Figure 1.3. In order to design a stable feedback system, and properties such as transient overshoot, settling time, and steady state regulation should meet special demands, and the model of converter should be established first. The dynamic model of a DC–DC converter can be one of several [2, 4]:

1. circuit model,
2. linearized model,
3. state-space model and averaged state-space model,
4. discrete time sampled data model.

The state-space model is the most popular among those mentioned above, and is the key step in modeling PWM converters with the small-signal linearization model. We will use the buck converter to illustrate the state-space modeling method of DC–DC converters.

A *state-space model* is a model of a system that may be represented by a differential equation. Here the state is a collection of variables summarizing the past of a system for the purpose of predicting the future. The system is called time-invariant if the



different equations do not explicitly depend on time t . However, it is possible to have more general time-varying systems because the functions depend on time.

A system is called linear if the functions are linear in \mathbf{x} and u . A linear state-space system can thus be represented as state equations in the matrix forms of

$$\begin{cases} \dot{\mathbf{x}} = A\mathbf{x} + Bu \\ y = C\mathbf{x} + Du \end{cases} \quad (1.2)$$

where \mathbf{x} is the *state variables*, which are a minimum number of variables to uniquely specify the state of the system, u is the independent input to the system, A , B , C , and D are constant matrices. Such a system is said to be *linear time invariant (LTI)*.

For the buck DC–DC converter, choosing the inductor current and capacitor voltage as natural state variables, and picking the input voltage source as u and resistor voltage as the output v_o , there are two state matrices for CCM operation based on the circuit theory.

Mode 1: Switch S is on, at duration dT :

$$\begin{cases} \dot{\mathbf{x}} = A_1\mathbf{x} + B_1u \\ v_o = C_1\mathbf{x} \end{cases} \quad (1.3)$$

Mode 2: Switch S is off, at duration $(1-d)T$:

$$\begin{cases} \dot{\mathbf{x}} = A_2\mathbf{x} + B_2u \\ v_o = C_2\mathbf{x} \end{cases} \quad (1.4)$$

Here, $\mathbf{x} = [v_o \ i_L]^T$, $A_1 = A_2 = \begin{pmatrix} 0 & -\frac{1}{L} \\ \frac{1}{C} & -\frac{1}{RC} \end{pmatrix}$, $B_1 = [1/L \ 0]^T$, $B_2 = [0 \ 0]^T$, and $C_1 = C_2 = [0 \ 1]^T$.

The *state-space averaged model* is a method of deriving the average value of state variables in one period. For switching converters, averaging and weighting the state variables by duty cycle over a switching period T , we obtain a state-space averaged equation

$$\begin{cases} \dot{\mathbf{x}} = [A_2d + A_1(1-d)]\mathbf{x} + [B_1d + B_2(1-d)]u \\ v_o = [C_1d + C_2(1-d)]\mathbf{x} \end{cases} \quad (1.5)$$

Next, disturbance and linearization methods are utilized near the working points to obtain a small-signal model. Finally, the transfer function may be obtained using the small-signal model to design the linear controller through classic control theory.

Generally speaking, although the proponents of a given method may prefer to express the end result in a specific form, the end results of nearly all methods are equivalent.



1.2.5 Discrete Model of DC–DC Converters

Under the assumption of a converter operating in a small range beside the steady-state working points, linear models are used extensively to describe the dynamics of a system. However, when a system is required to operate over a large range, in most cases, linear models do not provide satisfactory descriptions of the system's behavior. The discrete model is a kind of large signal model.

If we observe the representative points of every fixed interval, unlike the continuous motions of the orbits in phase plane, a series of discrete points may be obtained. And studying the motion of the orbits comes down to the motion of discrete points. The time interval is called the sampling period, and the discrete points are called sampling points. Mapping by sampling constant time intervals is called *stroboscopic mapping*.

Example 1.1 A Boost Converter A schematic diagram of a peak-current control boost converter is shown in Figure 1.9. The current waveform is illustrated in Figure 1.10. It is assumed that the boost converter is working in CCM, so that the inductor current never falls to zero. When the current through inductor L reaches the reference peak current I_{ref} , the comparator outputs a high level voltage which may reset the RS-flipflop to a low voltage and drive the switch S off, while the inductor releases energy that makes the inductor current decrease. When the next clock pulse comes, the RS-flipflop will be set to a high voltage and drive the switch S on to restore energy to the inductor, and the inductor current increases.

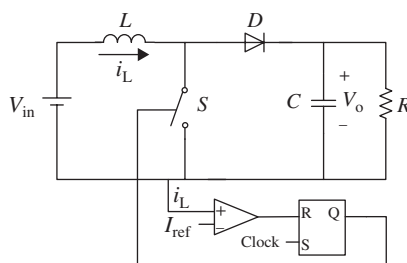


Figure 1.9 Schematic diagram of boost converter of peak-current control

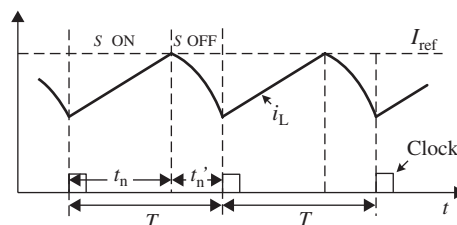


Figure 1.10 Current waveform of peak-current control



Stroboscopic maps relate the time-discrete state vector at every clock instant [19, 20]. Let i_L and v_C at the n th switching moment be i_n and v_n respectively, and those at the next moment be i_{n+1} and v_{n+1} respectively. We get

$$x_{n+1} = \begin{cases} e^{A_2(T-d_n T)} \left(e^{A_1 d_n T} x_n + \int_0^{d_n T} e^{A_1(d_n T - \tau)} d\tau B_1 E \right) \\ \quad + \int_{d_n T}^T e^{A_2(T-d_n T - \tau)} d\tau B_2 E & d_n < T \\ e^{A_1 T} x_n + \int_0^T e^{A_1(T-\tau)} d\tau B_1 E & d_n \geq T \end{cases} \quad (1.6)$$

If A_1 and A_2 are all full rank,

$$x_{n+1} = \begin{cases} e^{A_2(T-d_n T)} \left[e^{A_1 d_n T} x_n + (e^{A_1 d_n T} - I) A_1^{-1} B_1 E \right] \\ \quad + (e^{A_2(T-d_n T)} - I) A_2^{-1} B_2 E & d_n < T \\ e^{A_1 T} x_n + (e^{A_1 T} - I) A_1^{-1} B_1 E & d_n \geq T \end{cases} \quad (1.7)$$

Using Equation 1.7, the stroboscopic map of a peak-current control boost converter is [27]:

$$\begin{cases} i_{n+1} = e^{-kt'_n} (A_1 \sin \omega_1 t'_n + A_2 \cos \omega_1 t'_n) + E/R \\ v_{n+1} = E + e^{-kt'_n} [(A_1 kL + A_2 \omega_1) \cdot \sin \omega_1 t'_n + (A_2 k - A_1 \omega_1) L \cos \omega_1 t'_n] \end{cases} \quad (1.8)$$

where, $k = 1/2RC$, $\omega_1 = \sqrt{1/LC - R^2}$, $t_n = L(I_{\text{ref}} - i_n)/E$, $t'_n = T - t_n$, $A_1 = \frac{kL(I_{\text{ref}} - E/R) + E - v_n e^{-2kt_n}}{\omega_1 L}$, and $A_2 = (I_{\text{ref}} - E/R)$.

In this example, the sampling time instants of the stroboscopic map are synchronous with the switching events, thus it is also called a *stroboscopic switching map*. Moreover, for voltage-mode control DC-DC converters, there is always a special phenomenon called the *skipped cycle* in the case that the control voltage is beyond the ramp voltage. Fortunately, S-switching and A-switching maps are utilized to model DC-DC converters for this particular situation. Detailed introductions to S-switching and A-switching maps are described in [28], and they are not presented again in our book.

1.3 Overview of the Nonlinear Behavior of DC-DC Converters

In this section, we will take a look at the nonlinear phenomena that govern the complex motion of DC-DC converters. Studies of the nonlinear behavior of power electronic converters began with DC-DC converters over the past 30 years. In 1984, the chaos phenomenon of the buck converter was first mentioned by Brockett and Wood [29]. Hamill and Jefferies [30] introduced bifurcation and chaos in a PWM buck converter, where the difference equations and return maps were utilized to analyze its stability domain in 1988. The phenomena of boundedness, intermittency, and chaos were then



observed in an experiment by Krein and Bass in 1990 [31]. From then on, plenty of complex behavior was discovered in power electronic converters.

We give an example of a boost converter in peak current control in Figure 1.9 to illustrate several basic methods and the usual nonlinear behavior of DC–DC converters.

A *phase portrait* is a collection of trajectories that represents the solutions of equations in the state-space. For instance, using the parameters provided gives an example of phase portraits corresponding to time domain waveforms as shown in Figure 1.11 [27].

A qualitative change in the number of solutions to a dynamical system by varying a parameter is called a *bifurcation*. A *bifurcation diagram* is a graphical representation of bifurcation: a parameter is varied and plotted along the x -axis, and the asymptotic

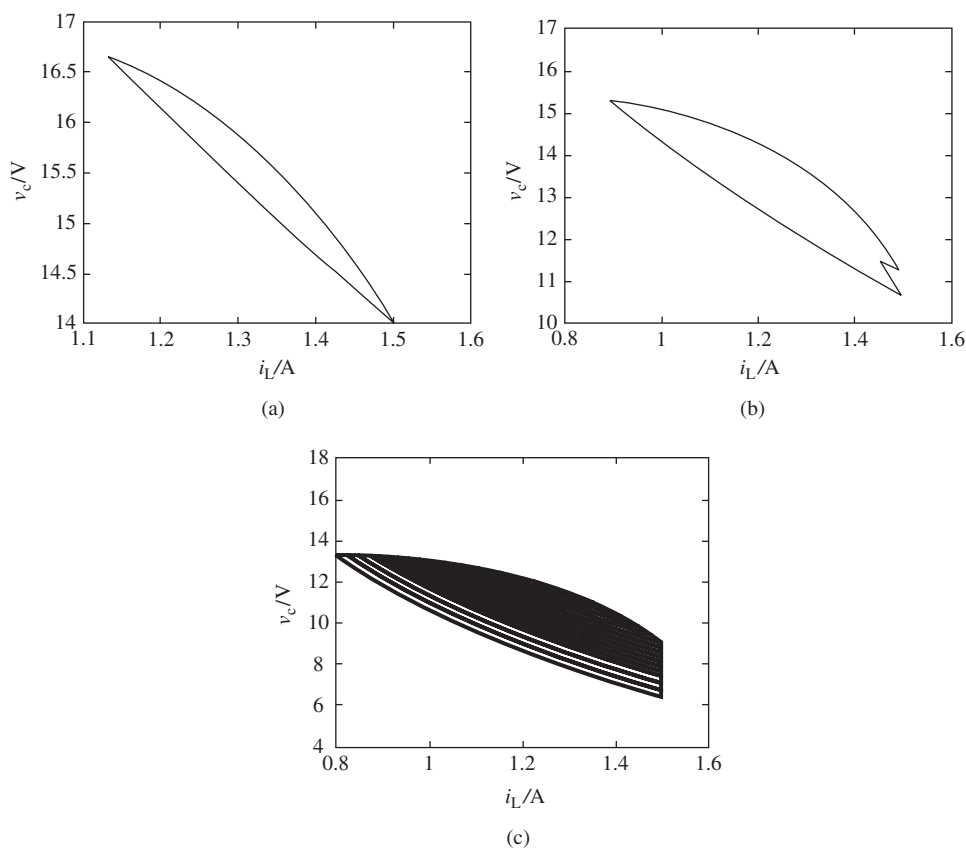


Figure 1.11 Phase portraits of (a) period-1, (b) period-2, and (c) chaos. Reprinted, with permission, from Deane, J.H.B, Chaos in a current-mode controlled dc-dc converter, IEEE Trans. Circuits Syst. I, and Aug./1992



behavior of a sampled state variable is plotted on the y -axis as discrete points [28]. A bifurcation diagram of a boost converter is shown in Figure 1.12. If the system is operating in period-1 for some parameter values corresponding to a cycle in the phase portrait, there will be only one point in the bifurcation diagram. If it is in period-2, there will be two points. Such a bifurcation diagram summarizes the change in system behavior in response to the variation of a parameter [28].

Decreasing the value of converter's input voltage E , the system successively undergoes period-1, period-2, period-4, ..., period- $2n$ (n is the positive integers) and chaotic orbits as shown in Figure 1.12. The discrete points filled in in the bifurcation diagram are obtained by sampling the inductor current i every T time interval repeatedly, where T is the switching period.

In this converter, there are two kinds of bifurcations, period-doubling bifurcation and border-collision bifurcation. Period-doubling bifurcation is a smooth and standard bifurcation, whose period number increases multiply as period-1, period-2, period-4, and so on, which is common in buck or boost converters with current-mode controlled and voltage-mode controlled [18].

As we know, for DC-DC converters, the duty cycle of a switch is limited in 0–1. Suppose that the converter operates in CCM; three kinds of possible current waveforms within one clock period T with the current-peak controlled are shown in Figure 1.13. The stable current waveform usually undergoes two working modes, mode 1 and mode 2, introduced previously, Figure 1.13a, where its duty cycle is $0 < d < 1$. There is another unsteady state presented in Figure 1.13b, where only mode 1 appears, and whose duty cycle d is saturated and equals 1. If the current waveform just touches the reference current at the end of clock T , Figure 1.13c, it is a boundary situation between Figure 1.13a,b. The border-collision bifurcation exists due to the saturation of the duty cycle, and occurs when duty cycle d reaches one of the saturation values 0 or 1. This type of bifurcation occurs in dynamical

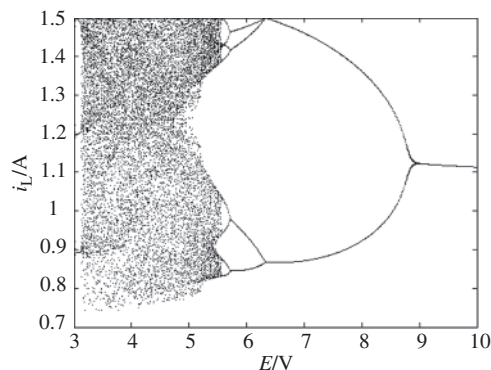


Figure 1.12 Bifurcation diagram of boost converter under peak-current control. Reprinted, with permission, from Deane, J.H.B, Chaos in a current-mode controlled dc-dc converter, IEEE Trans. Circuits Syst. I, and Aug./1992

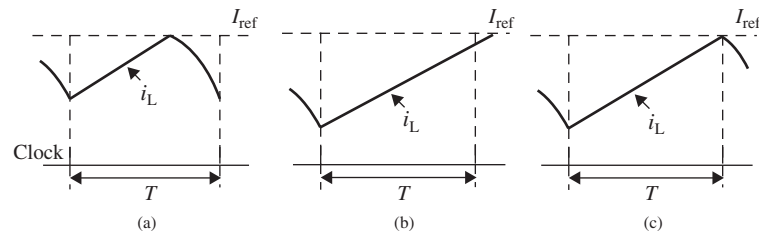


Figure 1.13 Modes of CCM of peak-current control at (a) $0 < d < 1$, (b) $d = 1$, and (c) boundary situation

systems where two or more structurally different systems operate for different parameter ranges [18]. Mathematically, when orbits of a piecewise-smooth system (introduced subsequently) tangent to some borders, this bifurcation will occur. We might distinguish this for the transform from period-2 to period-4, there is an unsmooth curve-like fold at the top of the bifurcation diagram which means the appearance of border-collision bifurcation. Of course, border-collision bifurcation is a nonstandard bifurcation.

In Figure 1.11c, we find the trajectory appears to move randomly in the state-space. Moreover, the trajectory is bounded and the motion is nonperiodic [18], or termed bounded aperiodic orbits. In the bifurcation diagram, we also find that there are plenty of populated points (infinite theoretically), which look like snow on a television set. We may roughly discover some properties as follows: (i) it looks random because the points are dense and chaotic (ii) but, it is ordered because the points concentrate in a certain bound. Roughly speaking, trajectories of the system that start in a particular bounded region of the state-space (known as *chaos* or *strange attractor*) will forever remain in that region, without exhibiting any apparent regularity or pattern (e.g., without converging to an equilibrium or becoming periodic).

1.4 Review of Basic Dynamics Concepts

Since Newton mechanics was founded, people have firmly believed that if a deterministic input is imposed on a deterministic dynamical system, then the output of the system must be determined as well. For the linear system, this conclusion is quite correct, but for the nonlinear system, some motions that may not be precisely repeated and are seemingly random may emerge.

Unfortunately, PWM DC–DC converters are none other than this kind of nonlinear system. The usage of semiconductor switches means that PWM DC–DC converters represent a hybrid system, which involves both continuous-valued and discrete-valued variables. Therefore, due to the nature of the switching process, PWM DC–DC converters are not a continuously differentiable system nor a nonsmooth system, which may give rise to complex dynamics. In this section, we will start with some basic



concepts of a dynamical system from dynamics theory. This material is available in many textbooks on nonlinear dynamics [33–37]. So we shall always try to present their concepts in geometrical images for ease of understanding.

1.4.1 Dynamical System

Roughly speaking, a dynamical system describes the evolution of a state over time. The evolution rule of the dynamical system is a fixed rule that describes what future states follow from the current state. According to the form of state evolution, dynamical systems can be classified into:

1. *continuous-time dynamical systems* and
2. *discrete-time dynamical systems*.

1.4.1.1 Continuous-Time Dynamical System

The state of continuous-time dynamical systems is allowed to change (continuously or discontinuously) at all times t . *Ordinary differential equations (flows)* are employed to describe continuous-time dynamical systems. A generalized continuous-time dynamical system is governed by the state-space model in vector form

$$\dot{\mathbf{x}} = f(\mathbf{x}, t) \quad (1.9)$$

where \mathbf{x} is the real, n th-order state vector in \mathbb{R}^n . $\dot{\mathbf{x}}$ is called a vector field, it gives a vector pointing in the direction of the velocity at every point in phase space.

If there is no time term t at the right hand side of Equation 1.9

$$\dot{\mathbf{x}} = f(\mathbf{x}) \quad (1.10)$$

this is called a form of *autonomous system*. For the actual system, it means that the system does not have any externally applied time-varying input or other time variation. For example, a three-dimensional Lorenz system is

$$\begin{cases} \dot{x}_1 = a(x_1 - x_2) \\ \dot{x}_2 = (1 + b)x_3 - x_2 - x_1x_3 \\ \dot{x}_3 = x_1x_2 - cx_3 \end{cases} \quad (1.11)$$

where a, b, c are parameters.

Conversely, Equation 1.9 is a *nonautonomous system* which has external inputs or forcing functions or time variations. For example, PWM power electronic circuits are explicitly time-dependent nonautonomous systems whose operations are compulsively controlled by clock logic with period T .

For a continuous-time dynamical system, the basic geometrical objects associated with a dynamical system are its orbits in the state-space and the phase portrait composed of these orbits.



Equilibrium: Consider the autonomous system, a state $\mathbf{x}^* \in \mathbb{R}^n$ is called an equilibrium of Equation 1.9 if $f(\mathbf{x}^*) = 0$.

Cycle: A cycle is periodic orbit for a vector field, namely a nonequilibrium orbit.

Limit cycle: A cycle of a continuous-time dynamical system, in a neighborhood of which there are no other cycles, is called a limit cycle [31].

Obviously, a limit cycle is the periodic solution with period T satisfying the equation

$$x(t + T) = x(t)$$

The trajectory in phase-space is a point or a closed curve, and is called an equilibrium or limit cycle as shown in Figures 1.14a,b respectively. Physically, the stable limit cycle is called self-oscillation.

1.4.1.2 Discrete-Time Dynamical Systems

The state of discrete-time dynamical systems can only change at discrete time instances. Difference equations are employed to describe discrete-time dynamical systems. In some circumstances, it is more natural to describe the evolution of a system at discrete instants of time rather than continuously in time, for example, in ecology and economics when the state of a system at a certain moment of time t completely determines its state after a year, say at $t + 1$. Discrete time refers to the set of times that is a subset of the integers. We will use $n \in \mathbb{Z}$ to denote discrete time. Typically, the evolution of the state of a discrete time system with a control parameter is expressed by a difference equation [33, 37]

$$\mathbf{x}_{n+1} = f(\mathbf{x}_n, \mu) \quad (1.12)$$

where \mathbf{x} is the n th-dimension state variable, μ is the set of all control variables, and this equation also may be called a map f , written as $x \mapsto f(x)$.

A *fixed point* of the discrete-time dynamical system is \mathbf{x}^* such that $\mathbf{x}^* = f(\mathbf{x}^*, \mu)$. Defining $f^n(\mathbf{x}_0)$ is the result of n times iterations of Equation 1.12 from an initial \mathbf{x}_0 . If finally $f^n(\mathbf{x}_0) = \mathbf{x}_0$, and for an arbitrary integer $k < n$, $f^k(\mathbf{x}_0) \neq \mathbf{x}_0$ is always satisfied,

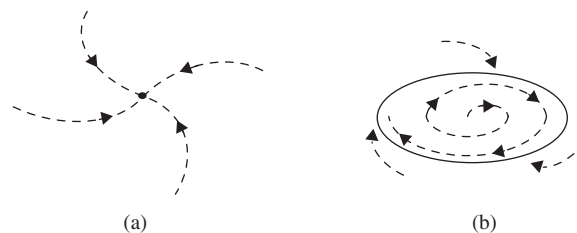


Figure 1.14 Illustration of stable (a) equilibrium and (b) limit cycle in a continuous-time system

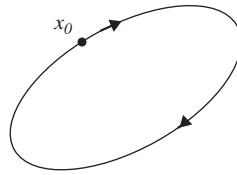


Figure 1.15 Periodic orbits in a discrete-time system

then set $\{\mathbf{x}_0, f(\mathbf{x}_0), \dots, f^{n-1}(\mathbf{x}_0)\}$ is a period- n orbit of map f . Using a geometrical point of view on dynamical systems, the period orbit of a discrete-time dynamical system is plotted in Figure 1.15.

1.4.2 Linear and Nonlinear Dynamical Systems

Dynamical systems can be further classified according to the equations used to describe the evolution of their state

1. *Linear dynamical system*, if the evolution is governed by a linear differential equation (continuous time) or difference equation (discrete time). Linear dynamical systems can be solved in terms of simple functions, and the behavior of all orbits is classified.
2. *Nonlinear dynamical system*, if the evolution is governed by a nonlinear differential equation (continuous time) or difference equation (discrete time). For example, the aforementioned Lorenz system is a nonlinear continuous-time system.

The theory of linear systems is mature and well developed. Many problems in linear systems theory have been solved using readily available mathematical tools. On the other hand, periodic solutions of nonlinear system are rarely known analytically. But, the study of nonlinear systems is important because almost every real system contains nonlinearities of one form or another [38].

Although there are types of nonlinear systems in mathematics and practical engineering, we will focus on piecewise linear systems because DC–DC converters are naturally modeled as piecewise smooth systems.

1.4.2.1 Piecewise-Smooth Dynamical Systems

The map is *smooth* when the map is continuously differentiable within the whole domain. In mathematics, a piecewise-defined function is defined by multiple sub-functions, and each sub-function applies to a certain interval of the main function's domain (a sub-domain). The map is called *piecewise-smooth* if it has the following two properties: (i) the state-space is divided into different sub-domains, and each sub-domain has independent map expressions and (ii) the map is continuous



in the whole state-space, is piecewise continuously differentiable in different sub-domains, and is not differentiable at the boundaries.

The piecewise-smooth dynamical system may switch between different sub-domains, because the system state trajectories may cross one of the state-space boundaries. Undoubtedly, a piecewise-smooth dynamical system is nonlinear dynamical system. There are three classes of piecewise-smooth systems: maps, flows, and hybrid systems [34].

1.4.2.2 Hybrid Dynamical Systems

Hybrid dynamical systems are combinations of maps and flows, giving rise to discontinuous, piecewise-smooth flows. They can arise both as models of impacting systems or in the context of the interaction between digital and analog systems. For example, hybrid automata [35] are defined as dynamical systems with a discrete and a continuous part. The discrete dynamics can be represented as a graph whose vertices are the discrete states (or modes) and whose edges are transitions. The continuous states take values in \mathbb{R}^n and evolve along trajectories, typically governed by ODEs or differential algebraic equations. The interaction between the discrete and the continuous dynamics takes place through invariants and transition relations [34].

For example, a PWM boost converter under peak current control (Figure 1.10) is considered. There are three operation modes, or three topologies, Mode 1, Mode 2, and Mode 3, corresponding to $(S, D) = (\text{on}, \text{off})$, $(S, D) = (\text{off}, \text{on})$, and $(S, D) = (\text{off}, \text{off})$, respectively. Figure 1.16 is the hybrid model of the converter. These topologies are a definitely continuous system and may be described by ordinary differential equations. However, converters are designed to work in these two or three topologies cyclically (CCM or DCM), and the transform from one topology to another is controlled by the external driving signal, which is a typical digital signal or discrete-valued. Therefore, DC–DC converters are definitely piecewise-smooth hybrid systems which include continuous and discrete systems synchronously. Therefore, they may have complex nonlinear behavior.

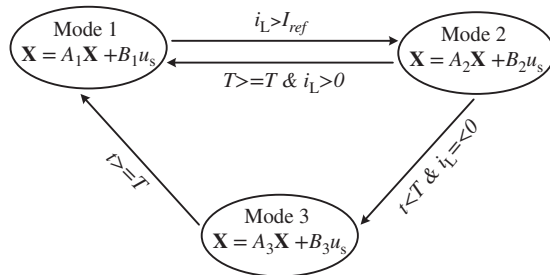


Figure 1.16 Hybrid model of a boost converter in peak-current control



1.4.3 Characterization of Nonlinear Behavior

It is well known that linear methods applied alone cannot give a reasonable explanation of nonlinear phenomena. Thus, some mathematical tools, including phase portraits, bifurcation diagrams, Lyapunov exponents (LEs), power spectrums, Poincaré Sections, Jacobian matrices, spider diagrams, and so on, provide information about the dynamics of the nonlinear dynamical system.

1.4.3.1 Poincaré Map

DC–DC converters are a type of hybrid system managed by a close-loop feedback controller. It is difficult to obtain the analytical solution, even a numerical solution, so some graphical tools are used to analyze these systems. In the previous section, we introduced phase portrait and bifurcation diagrams to describe several motions of a dynamical system. Compared with analytical methods, these methods may simplify complex nonlinear behavior. However, for instance, some periodic motions have high period numbers which perhaps are a mess and difficult to distinguish from aperiodic trajectories. A common mathematical tool called the Poincaré section can solve this question well.

A Poincaré section is a hypersurface Σ in the state-space, which replaces state trajectories of the n -dimensional continuous vector field with an $(n - 1)$ -dimensional map as shown in Figure 1.17. When this plane has a finite number of fixed points, the original continuous trajectories are periodic. When this plane has a closed curve, the original continuous trajectories are quasi-periodic. When the plane has dense points assembling in a certain zone, the original trajectories are chaotic. It is difficult to obtain the analytical solutions or numerical solutions of the majority of nonlinear continuous-time systems, so the intuitive features of the Poincaré section make the relevant studies convenient.

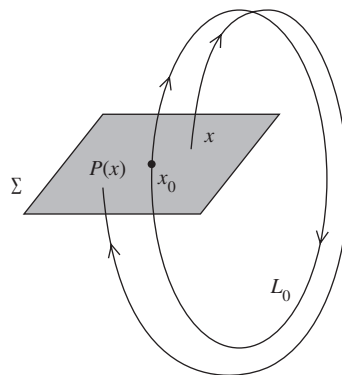


Figure 1.17 Illustration of Poincaré section. With kind permission from Springer Science+Business Media: Applied Mathematical Sciences, “Elements of Applied Bifurcation Theory”, 112, ©2000, Kuznetsov, Y. A.



If we observe the representative points at every constant time interval, unlike the continuous motions of the orbits in phase plane, a series of discrete points may be obtained. Studying the motion of the orbits comes down to the motion of discrete points, or a new discrete-time system, or Poincaré map. As already mentioned, the time interval is called the sampling period, the discrete points are called the sampling points, and the new map is called the stroboscopic map. The discretized system thus reveals the periodicity of the orbit of the underlying continuous-time system via the periodicity of the corresponding sampled state.

Next, a buck converter is used as an illustration to describe the chaos motions via the Poincaré map. The buck converter is in voltage control with parameters $L = 20$ mH, $C = 47$ μ F, $A = 8.4$, $V_L = 3.8$ V, $V_U = 8.2$ V, $T = 400$ μ s, $R = 22$, and $V_{\text{ref}} = 11.3$ V as shown in Figure 1.18. The discrete map is modeled according to Equation 1.8, and the Poincaré Section of the inductor current and capacitor voltage at fixed time intervals T is obtained using the discrete map. Figures 1.19a and b show the period-1 and period-2 orbits at $E = 22$ V and $E = 28$ V respectively. The Poincaré Section with $E = 37$ V is shown in Figure 1.19c. The left one is the corresponding phase portrait, and the right is the trajectories plotted as graphs of v and v_{ramp} . From this figure, there are contiguously populated regions, proving that the converter is chaotic.

1.4.3.2 Power Spectrum

Nonrandom motions have a definite frequency structure, and Fourier analysis is a tool to determine the frequency contents of a given signal. If the signal is periodic or quasi-periodic, the power spectrum will consist of a sequence of “spikes” at the fundamental frequencies. If the signal is neither periodic nor quasi-periodic (for example, it is chaotic), then the spectrum will be continuous. Thus, the sudden appearance of a continuous power spectrum from a discrete spectrum is viewed as an indicator of the onset of chaotic behavior when some parameters of the system are changed [40].

A power spectrum is very useful for analysis of a time series, especially for experiment and simulation data. For example, Feigenbaum (1976) used power spectrum

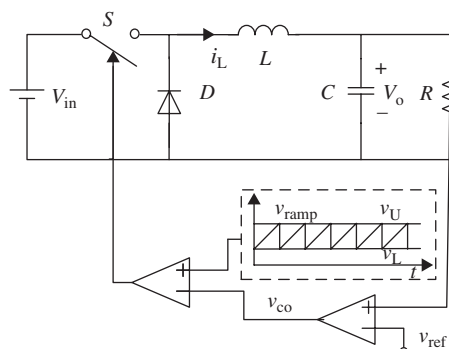


Figure 1.18 Schematic diagram of buck converter

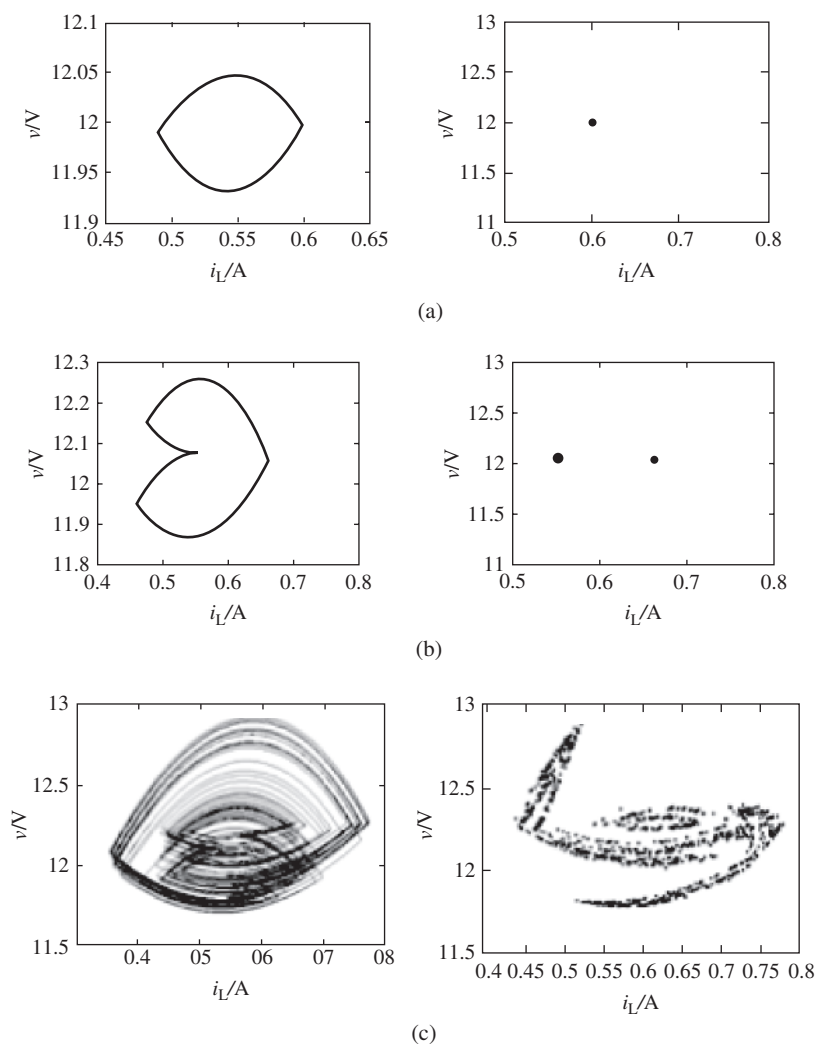


Figure 1.19 Phase portrait and Poincaré section of buck converter for (a) $E = 22$, (b) $E = 28$, and (c) $E = 37$ V

analysis to study the onset spectrum of turbulence [36]. Next, Gollub and Bension used it in a turbulent convection study [37], and it was then used in the study of non-linear behavior of the Josephson junction by Iansiti *et al.* [41], and so on.

The spectrum structure of period-doubling bifurcation and chaos is illustrated in Figure 1.20, where the higher harmonics are ignored. For period-1 motion, the spectrum is dominated by a primary spectral peak with f_0 . For period-2 motion, the subharmonic ($f_0/2$) is excited beside the primary spectral peak. For period-4 motion, the spectrum contains four peaks, corresponding to a new subharmonic ($f_0/4$).

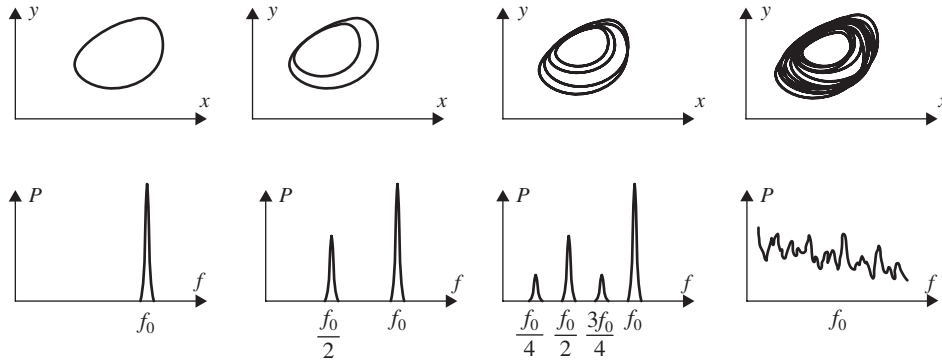


Figure 1.20 Power spectrum of period-doubling bifurcation. From left to right, there are phase trajectories and spectrums of period-1, period-2, period-4, and chaos

When the system becomes chaotic, the spectrum has broadband and continuous characteristics. In other words, chaos motion may be characterized by the presence of broadband and a continuous power spectrum.

1.4.3.3 Jacobian Matrix

The Jacobian matrix is another commonly used mathematic tool aside from the Poincaré map, which is used to analyze the stability of equilibriums or fixed points in continuous or discrete systems.

Suppose that a continuous smooth dynamical system has the form of

$$\begin{cases} \dot{x} = f_1(x, y) \\ \dot{y} = f_2(x, y) \end{cases} \quad (1.13)$$

and x_0, y_0 are its equilibriums. The Jacobian matrix of Equation 1.13 is given by

$$\mathbf{J} = \begin{pmatrix} \frac{\partial f_1}{\partial x} & \frac{\partial f_1}{\partial y} \\ \frac{\partial f_2}{\partial x} & \frac{\partial f_2}{\partial y} \end{pmatrix} \Big|_{\substack{x=x_0 \\ y=y_0}} \quad (1.14)$$

Assuming that Matrix \mathbf{J} has two eigenvalues λ_1 and λ_2 , which are the roots of the characteristic equation

$$\lambda^2 - \sigma\lambda + \Delta = 0 \quad (1.15)$$

where $\sigma = \text{tr}(\mathbf{J})$, $\Delta = \text{det}(\mathbf{J})$. The eigenvalues of this matrix determine the stability of the equilibriums. A stable equilibrium attracts nearby trajectories, while an unstable equilibrium repels nearby trajectories. Eigenvalues λ_1 and λ_2 might be real or complex numbers, whose values indicate the classification of equilibrium and fixed points. For detailed classification, please see references [33, 35]. Generally speaking,



in the dynamical system, all eigenvalues of the Jacobian matrix will motion on the complex plane with a certain parameter. When the change parameter (called a bifurcation parameter) reaches a critical value, the stability of a periodic orbit changes and bifurcation behavior occurs.

Now we consider a discrete-time dynamical system

$$x \mapsto f(x) \quad x \in \mathbb{R}^n \quad (1.16)$$

where the map f is smooth. Let $x_0 = 0$ be a fixed point of the system (i.e., $f(x_0) = x_0$) and let \mathbf{J} denote the Jacobian matrix df/dx evaluated at x_0 . The eigenvalues $\lambda_1, \lambda_2, \dots, \lambda_n$ of \mathbf{J} are called *multipliers* or *Floquet multipliers* of the fixed point. The absolute values of multipliers may be determined. When all $|\lambda| < 1$, the fixed points are stable. When $|\lambda| > 1$, the fixed points are unstable. Thus, the bifurcation appears at the *Floquet unit circle* ($\lambda = \pm 1$). The standard bifurcation types of discrete system, such as tangent bifurcation, period-doubling bifurcation, and torus bifurcation, may be distinguished by studying the trajectories of the multipliers. For the high dimension map, if all the multipliers are smaller than 1, the fixed points are stable. Conversely, as long as one multiplier is greater than 1, the fixed points are unstable. For power converters, the discrete map has the form

$$\mathbf{x}_{n+1} = f(\mathbf{x}_n, d_n, \mu_n) \quad (1.17)$$

where \mathbf{x} is the state variable, μ_n is the system parameter, d_n is the duty cycle, and the subscript n defines the n th switching period. The stability of the map may be estimated by the characteristic values of the Jacobian matrix. The relationship between d_n and x_n can be expressed using the *switching surface*

$$s(\mathbf{x}_n, d_n) = 0 \quad (1.18)$$

The Jacobian matrix of Equation 1.17 is

$$J(\mathbf{x}^*) = \frac{\partial f}{\partial \mathbf{x}_n} - \frac{\partial f}{\partial d_n} \left(\frac{\partial s}{\partial d_n} \right)^{-1} \frac{\partial s}{\partial \mathbf{x}_n} \Big|_{\mathbf{x}_n = \mathbf{x}^*} \quad (1.19)$$

And the eigenvalues are roots of the characteristic equation

$$\det[\lambda I - J(\mathbf{x}^*)] = 0 \quad (1.20)$$

where I is the $n \times n$ identity matrix. When the maximum value of the norms of the characteristic roots λ is greater than 1, Equation 1.17 will not be convergent and the unstable phenomenon will occur.

1.4.3.4 Lyapunov Exponents

Although power spectrum is an intuitive and graphic method, it is not a characteristic quantity of “invariance” in principle. For example, to calculate the power spectrum, the signal $\{x_i\}$ should be changed to $\{x_i^2\}$. Hence, some new frequency components will appear naturally.



LEs are quantitative measures of the evolution of the phase trajectories, and are useful for distinguishing chaos and non-chaos. As we all know, the basic performance of chaos is sensitivity to initial conditions. Eigenvalues of the Jacobian matrix decide the rate of being stretched or expanded of two local neighbor trajectories, but this rate is perhaps different for the other neighbor trajectories in the whole phase space. Therefore, it is very necessary to quantify the overall characteristics of the dynamical system, and LEs are one of the quantity parameters (invariant measures, fractal dimension, etc., are the others). In mathematics, *Lyapunov exponents* are defined as an average rate of exponential divergence of two initially nearby trajectories. Quantitatively, two trajectories in phase space with initial separation δx_0 diverge (provided that the divergence can be treated within the linearized approximation) at a rate given by

$$|\delta x(t)| \approx e^{\lambda t} |\delta x_0| \quad (1.21)$$

where λ is the LE.

What is a geometrical meaning of LEs? The theory is illustrated in Figure 1.21. Consider two points in a phase space, x_0 and $x_0 + \delta x_0$; each of them will generate an orbit using some equations. These orbits can be thought of as parametric functions of a variable like time. Because sensitive dependence can arise only in some portions of a system, this separation is also a function of the location of the initial value and has the form $\delta x(t)$. In a system with attracting fixed points or attracting periodic orbits, $\delta x(t)$ diminishes asymptotically with time. If a system is unstable, the orbits diverge exponentially for a while, but eventually settle down. For chaotic points, the function $\delta x(t)$ will behave erratically. It is thus useful to study the mean exponential rate of divergence of two initially close orbits using the formula

$$\lambda = \lim_{t \rightarrow \infty} \lim_{\delta x_0 \rightarrow 0} \frac{1}{t} \ln \frac{|\delta x(t)|}{|\delta x_0|} \quad (1.22)$$

This number is called the Lyapunov exponent, and there are three situations:

If $\lambda < 0$, the orbit attracts to a stable fixed point or stable periodic orbit.

If $\lambda = 0$, the orbit is a neutral fixed point (or an eventually fixed point). A LE of zero indicates that the system is in some sort of steady-state mode.

If $\lambda > 0$, the orbit is unstable and chaotic. Nearby points, no matter how close, will diverge to any arbitrary separation.

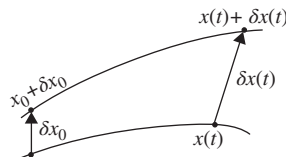


Figure 1.21 Geometrical meaning of Lyapunov exponents



LE is useful to distinguish among the various types of orbits. It works for discrete as well as continuous systems. We can legitimately conclude that the behavior of the system is chaotic only if its average LE is positive [40].

1.5 Conclusions

Switching converters are complex nonlinear, nonautonomous, and time varying systems, so they contain abundant nonlinear phenomena, such as chaos and bifurcation. First, we introduced the working principle and the basic topologies of the switching converters in this chapter. Second, an overview of nonlinear behavior in DC-DC converters was given. Finally, we introduced some reviews of basic nonlinear dynamics concepts, including the dynamical system and some characterizations of nonlinear behavior.

References

- [1] Rashid, M.H. (2004) *Power Electronics: Circuits, Devices, and Application*, 3rd edn, Pearson Education.
- [2] Agrawal, J.P. (2001) *Power Electronic Systems: Theory and Design*, Prentice-Hall, Upper Saddle River, NJ.
- [3] Erickson, R.W. and Maksimovic, D. (2000) *Fundamentals of Power electronics*, 2nd edn, Springer.
- [4] Rashid, M.H. (2007) *Power Electronics Handbook*, 2nd edn, Elsevier.
- [5] Luo, F.L. and Ye, H. (2004) *Advanced DC/DC Converters*, CRC Press.
- [6] Mohan, N., Undeland, T.M. and Robbins, W.P. (1995) *Power Electronics: Converters, Applications, and Design*, 2nd edn, John Wiley & Sons, Inc., New York.
- [7] Tse, C.K. (1994) Flip bifurcation and chaos in a three-state Boost switching regulators. *IEEE Trans. Circuits Syst. I*, **41**(1), 16–23.
- [8] Tse, C.K. (1994) Chaos from a Buck switching regulator operating in discontinuous mode. *Int. J. Circuits Theory Appl.*, **22**(4), 263–278.
- [9] Iu, H.H.C. and Tse, C.K. (2001) Bifurcation behaviour in parallel-connected Buck converters. *IEEE Trans. Circuit Syst. I*, **48**(2), 233–240.
- [10] Ma, Y., Tse, C.K., Kousaka, T. and Kawakami, H. (2005) Connecting border collision with saddle-node bifurcation in switched dynamical systems. *IEEE Trans. Circuit Syst. II*, **52**(9), 581–585.
- [11] Tse, C.K., Lai, Y.M. and Iu, H.H.C. (2000) Hopf bifurcation and chaos in a free-running current-controlled Ćuk switching regulator. *IEEE Trans. Circuit Syst. I*, **47**(4), 448–457.
- [12] Aroudi, A.E., Benadero, L., Toribio, E. *et al.* (1999) Hopf bifurcation and chaos from torus breakdown in a PWM voltage-controlled DC-DC boost converter. *IEEE Trans. Circuit Syst. I*, **46**(11), 1374–1382.
- [13] Iu, H.H.C. and Tse, C.K. (2003) Study of low-frequency bifurcation phenomena of a parallel-connected boost converter system via simple averaged models. *IEEE Trans. Circuit Syst. I*, **50**(5), 679–685.
- [14] Dai, D., Tse, C.K. and Ma, X. (2005) Symbolic analysis of switching systems: application to bifurcation analysis of DC-DC switching converters. *IEEE Trans. Circuits Syst. I Regul. Pap.*, **52**(8), 1632–1643.
- [15] Banerjee, S. (1997) Coexisting attractors, chaotic saddles, and fractal basins in a power electronic circuit. *IEEE Trans. Circuits Syst. I*, **44**(9), 847–849.



- [16] Wong, S.C., Tse, C.K. and Tam, K.C. (2004) Spurious modulation on current-mode controlled DC/DC converters: an explanation for intermittent chaotic operation. *IEEE ISCAS*, **5**, 852–855.
- [17] Tse, C.K., Zhou, Y., Lau, F.C.M. and Qiu, S. (2003) “Intermittent” chaos and subharmonics in switching power supplies. *IEEE ISCAS*, **3**, 332–335.
- [18] Tse, C.K. (2004) *Complex Behavior of Switching Power Converters*, CRC Press.
- [19] Aston, P.J., Deane, J.H.B., and Hamill, D.C. (1997) Targeting in systems with discontinuities, with applications to power electronics. *IEEE Trans. Circuits Syst. I*, **44**(10), 1034–1039.
- [20] Deane, J.H.B. and Hamill, D.C. (1996) Improvement of power supply EMC by chaos. *Electron. Lett.*, **32**, 1045–1045.
- [21] Morel, C., Bourcerie, M. and Chapeau-Blondeau, F. (2004) Extension of chaos anticontrol applied to the improvement of switch-mode power supply electromagnetic compatibility. *IEEE Int. Symp. Ind. Electron.*, **1**, 447–452.
- [22] Zhang, J.J., Zhang, L.M. and Qiu, S.S. (2006) An experimental investigation of EMI suppression of off-line switching converter by chaotic modulation. *Aerosp. Control*, **24**(4), 87–90.
- [23] Tse, K.K., Chung, H.S.-H., Huo, S.Y. and So, H.C. (2000) Analysis and spectral characteristics of a spread-spectrum technique for conducted EMI suppression. *IEEE Trans. Power Electron.*, **15**(2), 399–410.
- [24] Tse, K.K., Chung, H.S.-H., Huo, S.Y. and So, H.C. (2002) A comparative study of carrier-frequency modulation techniques for conducted EMI suppression in PWM converters. *IEEE Trans. Ind. Electron.*, **49**(3), 618–627.
- [25] Tse, K.K., Ng, R.W.-M., Chung, H.S.H. *et al.* (2003) An evaluation of the spectral characteristics of switching converters with chaotic carrier-frequency modulation. *IEEE Trans. Ind. Electron.*, **50**(1), 171–182.
- [26] Wang, X.M. (2008) Symbolic time series characterization and block entropy analysis of DC-DC converters. *Acta Physiol. Scand.*, **57**(10), 6112–6119.
- [27] Deane, J.H.B. (1992) Chaos in a current-mode controlled dc-dc converter. *IEEE Trans. Circuits Syst. I*, **39**(8), 680–683.
- [28] Banerjee, S. and Verghese, G.C. (2001) *Nonlinear Phenomena in Power Electronics: Attractors, Bifurcations, Chaos, and Nonlinear Control*, Wiley Press.
- [29] Brocckett, R.W. and Wood, J.R. (1984) Understanding power converter chaotic behaviour mechanisms in protective and abnormal modes. 11th Annual International Power Electronics, pp. 115–124.
- [30] Hamill, D.C. and Jefferies, D.J. (1988) Subharmonics and chaos in a controlled switched-mode power converter. *IEEE Trans. Circuits Syst. I*, **35**(8), 1059–1061.
- [31] Kuznetsov, Y.A. (2000) *Elements of Applied Bifurcation Theory*, 2nd edn, Springer-Verlag.
- [32] Wang, X.M., Zhang, B., and Qiu, D.Y. (2008) Bifurcations and chaos in H-bridge DC chopper under peak-current control. International Conference on Electrical Machines and Systems, 2008. ICEMS 2008, Wuhan, October 17–20, 2008, pp. 2173–2177.
- [33] Nayfeh, A.H. and Balachandran, B. (2004) *Applied Nonlinear Dynamics*, Wiley Press.
- [34] Bernardo, M., Budd, C.J., Champneys, A.R. *et al.* (2007) *Piecewise-smooth Dynamical Systems: Theory and Applications*, Springer-Verlag Press.
- [35] Branicky, M.S., Borkar, V.S. and Mitter, S.K. (1998) A unified framework for hybrid control model and optimal control theory. *IEEE Trans. Autom. Control*, **43**(1), 31–45.
- [36] Feigenbaum, M.J. (1980) The metric universal properties of period doubling bifurcations and the spectrum for a route to turbulence. *Ann. New York Acad. Sci.*, **357**, 330–336.
- [37] Gollub, J.P. and Benson, S.V. (1980) Many routes to turbulent convection. *J. Fluid Mech.*, **100**(3), 449–470.
- [38] Liu, D. and Michel, A.N. (1994) *Dynamical Systems with Saturation Nonlinearities*, Springer-Verlag Press.



- [39] Wang, X.M. (2009) *Study and Application of Bifurcation and Chaos Behavior of Power Electronic Converters Based on Discrete System Dynamics(in Chinese)*, South China University of Technology, Guangzhou.
- [40] Hilborn, R.C. (2000) *Chaos and Nonlinear Dynamics: An Introduction for Scientists and Engineers*, 2nd edn, Oxford University Press.
- [41] Iansiti, M., Hu, Q. and Westervelt, R.M. (1985) Noise and chaos in a fractal basin boundary regime of a Josephson junction. *Phys. Rev. Lett.*, **55**(7), 746–749.
- [42] Huang, R.S. and Huang, H. (2005) *Chaos and its Application (in Chinese)*, 2nd edn, Wuhan University Press.